Film Mode Matching Method for Photonic Crystal Slabs

Aasmund Sudbø University of Oslo
Graduate University Center - UniK
N-2027 KJELLER, Norway
email: aas@unik.no +47 6484 4700

April 12, 2005

Abstract

The film mode matching method for optical field calculations is applied to the calculation of Bloch wave fields in photonic crystal slab structures.

0.0.1 Introduction

Accurate calculation of electromagnetic field distributions in photonic crystals is of fundamental importance to the design of integrated optics and photonics. With the large differences in refractive index between the air, oxide and semiconductor materials that a photonic crystal is made from, a vector field description is needed. In this paper, a formalism is developed for the calculation of field distribution in a photonic crystal slab or slice surrounded by a homogeneous material on each side. The formalism is general enough to handle structures consisting of several parallell slices, possibly separated by slices of homogeneous material.

0.0.2 Numerical Methods

The method discussed here is an adaptation of the method used in (11; 8; 9; **?**) for computing the mode fields of optical waveguides. A structure analyzed with this method is modeled by a sandwich of M "slices" numbered $m = 1, 2...M$. Each slice is considered to be cut from a two-dimensional photonic crystal (PC). Hence it is natural to attach the label m to the PC that slice no. m is cut from, as well. A homogeneous material may be considered a special case of a PC. Our analysis requires all slices to have the same lattice structure and orientation.

Let us adhere to the common convention of having the homogeneous axis of the PCs as the z-axis. We also call the z-direction the longitudinal direction, and the x- and y-directions transverse directions. Then the slices are perpendicular to the z-axis, lying in the x-y-plane, as shown in Fig.1, and both the lattice vectors of the PCs and its reciprocal lattice vectors lie in the x-y-plane. We

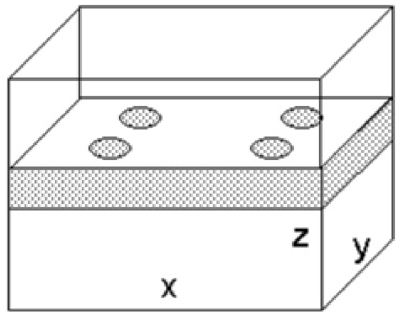

Figure 1: *Simple 3-slice structure consisting of air, a photonic crystal (PC) slice, resting on a homogeneous substrate. Four air holes are indicated in the PC, so two periods of the PC are shown in each direction.*

let both z and m increase from the bottom up. Let c be the speed of light, ω the angular frequency, λ the corresponding vacuum wavelength, and k the corresponding angular repetency, so that $k = \omega/c = 2\pi/\lambda$. Let $\hat{x}$, $\hat{y}$ and $\hat{z}$ denote unit vectors in the x-, y- and z-directions, respectively, let the position be $x\hat{x} + y\hat{y} + z\hat{z} = \vec{r} + z\hat{z}$, and let t denote time. Within slice no. m, we have Bloch wave (BW) solutions for the fields, where the x- and y-components of the E-field (the transverse components) may be written

$$\vec{E}\left(\vec{r}, z, t\right) = \vec{E}^{(m)}_{\vec{g},p}\left(\vec{k}, \omega, \vec{r}\right) \exp\left(i\vec{k}\cdot\vec{r} + ik^{(m)}_{\vec{g},p}\left(\vec{k}, \omega\right) z - i\omega t\right), \tag{1}$$

and correspondingly for the H-field. In the above equation, and in the following, an arrow above a symbol, like in $\vec{r} = x\hat{x} + y\hat{y}$, is used to denote a transverse vector, *i.e.*, a vector in the x-y-plane. The Block vector (BV) of the wave is

$$\vec{k} + k^{(m)}_{\vec{g},p}\left(\vec{k}, \omega\right)\hat{z}, \tag{2}$$

where $\vec{k}$ (the transverse BV) may be chosen freely in the first Brillouin zone of the photonic crystal (PC), if we adopt the reduced Brillouin zone scheme. The z-component $k_z = k^{(m)}_{\vec{g},p}\left(\vec{k}, \omega\right)$ of the BV must be calculated for each BW in slice no. m by solving Maxwells equations in photonic crystal no. m. For most purposes in the following, the subscript pair $(\vec{g}, p)$ may be considered just a label distinguishing the various BWs. For the limiting case of a homogeneous PC, *i.e.*, no spatial variation of ε and μ, the set of $\vec{g}$'s is the transverse reciprocal lattice vectors of the PC, and p represents two possible BW polarizations possible for each reciprocal lattice vector, *e.g.*, TE and TM.

The Block wave envelope fields (BWEFs) $\vec{E}^{(m)}_{\vec{g},p} + \hat{z}E^{(m)}_{z;\vec{g},p}$ and $\vec{H}^{(m)}_{\vec{g},p} + \hat{z}H^{(m)}_{z;\vec{g},p}$ are periodic functions of position $\vec{r}$, satisfying the following form of Maxwell's equations:

$$\left(\vec{\nabla}+i\vec{k}\right)\times\vec{E}^{(m)}_{\vec{g},p} = i\omega\mu\hat{z}H^{(m)}_{z;\vec{g},p}, \tag{3}$$

$$i\omega\varepsilon\vec{E}^{(m)}_{\vec{g},p} = \hat{z}\times\left[\left(\vec{\nabla}+i\vec{k}\right)H^{(m)}_{z;\vec{g},p} - ik^{(m)}_{\vec{g},p}\vec{H}^{(m)}_{\vec{g},p}\right], \tag{4}$$

$$\left(\vec{\nabla}+i\vec{k}\right)\times\vec{H}^{(m)}_{\vec{g},p} = -i\omega\varepsilon\hat{z}E^{(m)}_{z;\vec{g},p}, \tag{5}$$

$$\text{and}\quad i\omega\mu\vec{H}^{(m)}_{\vec{g},p} = -\hat{z}\times\left[\left(\vec{\nabla}+i\vec{k}\right)E^{(m)}_{z;\vec{g},p} - ik^{(m)}_{\vec{g},p}\vec{E}^{(m)}_{\vec{g},p}\right]. \tag{6}$$

From these equations it can be shown that

1. If we have an upward propagating Bloch wave (BW) with z-component $k_z = k^{(m)}_{\vec{g},p}\left(\vec{k},\omega\right)$ of the Block vector (BV), we also have a downward propagating BW with $k_z = -k^{(m)}_{\vec{g},p}\left(\vec{k},\omega\right)$, with the same transverse E-field, but with the transverse H-field inverted.

2. In a photonic crystal with inversion symmetry, for each k_z there is a pair of BWs with equal and opposite transverse BVs. For such a pair we may choose

$$\vec{E}^{(m)}_{\vec{g},p}\left(-\vec{k},\omega,\vec{r}\right) = \vec{E}^{(m)}_{-\vec{g},p}\left(\vec{k},\omega,-\vec{r}\right) \quad\text{and}\quad \vec{H}^{(m)}_{\vec{g},p}\left(-\vec{k},\omega,\vec{r}\right) = \vec{H}^{(m)}_{-\vec{g},p}\left(\vec{k},\omega,-\vec{r}\right).$$

3. In a PC with real ε and μ, a BWEF corresponding to an inversion of the transverse BV (from $\vec{k}$ to $-\vec{k}$) may be obtained by complex conjugation of the transverse E- and H-fields. If the PC also has inversion symmetry, then

$$\vec{E}^{(m)}_{\vec{g},p}\left(\vec{k},\omega,-\vec{r}\right) = \vec{E}^{(m)}_{-\vec{g},p}\left(\vec{k},\omega,\vec{r}\right)^* \quad\text{and}\quad \vec{H}^{(m)}_{\vec{g},p}\left(\vec{k},\omega,-\vec{r}\right) = \vec{H}^{(m)}_{-\vec{g},p}\left(\vec{k},\omega,\vec{r}\right)^*.$$

4. In a PC with real ε and μ, there are at least two BWs propagating in the z-direction, *i.e.*, with real k_z. (Two polarization states are always possible.) All the high-order BWs (those with large $|\vec{g}|$) are evanescent, *i.e.*, have purely imaginary k_z, increasing in absolute value with increasing order. The lower the frequency, the fewer propagating BWs there are. For a sufficiently low frequency, only two propagating BWs exist, and the remaining BWs are evanescent.

5. Even if ε and μ are real, in some PC structures k_z is actually complex in some frequency intervals (15). Complex conjugation then yields a BW with an inverted transverse BV and the complex conjugate z-component $k_z = k^{(m)*}_{\vec{g},p}$. If the PC also has inversion symmetry, there are 4 different BWs for a given $\vec{k}$, corresponding to $k_z = \pm k^{(m)}_{\vec{g},p}$ and $k_z = \pm k^{(m)*}_{\vec{g},p}$.

Comprising both upward- and downward-travelling BWs, the transverse E-field phasor in slice no. m may then be written as a sum of Bloch wave components:

$$\vec{E}^{(m)}(\vec{k},\omega,\vec{r},z) = \sum_{\vec{g},p} u_{\vec{g},p}^{(m)}(z)\ \vec{E}_{\vec{g},p}^{(m)}\left(\vec{k},\omega,\vec{r}\right) \exp\left(i\vec{k}\cdot\vec{r}\right), \tag{7}$$

and the corresponding transverse H-field phasor

$$\vec{H}^{(m)}(\vec{k},\omega,\vec{r},z) = -i\sum_{\vec{g},p} \left(\dot{u}_{\vec{g},p}^{(m)}(z)/k_{\vec{g},p}^{(m)}\right)\ \vec{H}_{\vec{g},p}^{(m)}\left(\vec{k},\omega,\vec{r}\right) \exp\left(i\vec{k}\cdot\vec{r}\right). \tag{8}$$

Let $z^{(m)}$ be the position of the interface between slices no. m and $m+1$, so that the thickness of slice no. m is

$$d_z^{(m)} = z^{(m)} - z^{(m-1)}, \tag{9}$$

and let the bottom slice be no. 1. The BW component amplitudes $u_{\vec{g},p}^{(m)}(z)$ then have the form

$$\begin{aligned} u_{\vec{g},p}^{(m)}(z) &= u_{\vec{g},p}^{(m,l,+)} \exp[ik_{\vec{g},p}^{(m)}(z-z^{(m-1)})] + u_{\vec{g},p}^{(m,l,-)} \exp[-ik_{\vec{g},p}^{(m)}(z-z^{(m-1)})] && (10)\\ &= u_{\vec{g},p}^{(m,l,E)} \cos[k_{\vec{g},p}^{(m)}(z-z^{(m-1)})] + iu_{\vec{g},p}^{(m,l,H)} \sin[k_{\vec{g},p}^{(m)}(z-z^{(m-1)})], && (11) \end{aligned}$$

with the z-derivatives

$$\begin{aligned} \dot{u}_{\vec{g},p}^{(m)}(z) &= ik_{\vec{g},p}^{(m)}u_{\vec{g},p}^{(m,l,+)} \exp[ik_{\vec{g},p}^{(m)}(z-z^{(m-1)})] - ik_{\vec{g},p}^{(m)}u_{\vec{g},p}^{(m,l,-)} \exp[-ik_{\vec{g},p}^{(m)}(z-z^{(m-1)})] && (12)\\ &= ik_{\vec{g},p}^{(m)}u_{\vec{g},p}^{(m,l,H)} \cos[k_{\vec{g},p}^{(m)}(z-z^{(m-1)})] - k_{\vec{g},p}^{(m)}u_{\vec{g},p}^{(m,l,E)} \sin[k_{\vec{g},p}^{(m)}(z-z^{(m-1)})]. && (13) \end{aligned}$$

In (10) and (11) $u_{\vec{g},p}^{(m,l,+)}$ and $u_{\vec{g},p}^{(m,l,-)}$ are the complex amplitudes of the BW components travelling upward and downward in slice no. m, at $z = z^{(m-1)}$, whereas $u_{\vec{g},p}^{(m,l,E)}$ and $ik_{\vec{g},p}^{(m)}u_{\vec{g},p}^{(m,l,H)}$ are the resulting total amplitudes and z-derivatives:

$$\begin{aligned} u_{\vec{g},p}^{(m,l,E)} &= u_{\vec{g},p}^{(m,l,+)} + u_{\vec{g},p}^{(m,l,-)} && (14)\\ \text{and}\quad u_{\vec{g},p}^{(m,l,H)} &= u_{\vec{g},p}^{(m,l,+)} - u_{\vec{g},p}^{(m,l,-)}. && (15) \end{aligned}$$

Using (10) and (11) we define corresponding amplitudes $u_{\vec{g},p}^{(m,u,\pm)}$, $u_{\vec{g},p}^{(m,u,E)}$ and $u_{\vec{g},p}^{(m,u,H)}$ on the upper side of slice no. m, at $z = z^{(m)}$. It will be convenient to have one symbol to represent either of the two slice side labels l and u; let us use the symbol s for this purpose.

One point to note about the BW expansions (7) and (8) is that they involve mostly evanescent BWs, since the higher-order BWs are all evanescent.

Then we are ready to introduce vectors $\mathbf{u}^{(m,s,\pm)}$, $\mathbf{u}^{(m,s,E)}$ and $\mathbf{u}^{(m,s,H)}$, with elements $u_{\vec{g},p}^{(m,s,\pm)}$, $u_{\vec{g},p}^{(m,s,E)}$, and $u_{\vec{g},p}^{(m,s,H)}$, respectively. Furthermore, we introduce diagonal matrices $\mathbf{K}^{(m)}$ with diagonal elements

$$K_{(\vec{g},p),(\vec{g},p)}^{(m)} = k_{\vec{g},p}^{(m)} d_z^{(m)}, \tag{16}$$

impedance matrices $\mathbf{Z}^{(m,s)}$ relating $\mathbf{u}^{(m,s;E)}$ and $\mathbf{u}^{(m,s;H)}$,

$$\mathbf{u}^{(m,s;E)} = \mathbf{Z}^{(m,s)} \mathbf{u}^{(m,s;H)}, \tag{17}$$

and reflection coefficient matrices $\mathbf{\Gamma}^{(m,s)}$ relating $\mathbf{u}^{(m,s,-)}$ and $\mathbf{u}^{(m,s,+)}$,

$$\mathbf{u}^{(m,s,-)} = \mathbf{\Gamma}^{(m,s)} \mathbf{u}^{(m,s,+)}, \tag{18}$$

Note that in these definitions we must group the upward decaying components (with positive imaginary $k_{\vec{g},p}^{(m)}$) together with the upward travelling BW components (with positive real $k_{\vec{g},p}^{(m)}$). This will become apparent in the discussion of boundary conditions below.

It is straightforward to show from (14), (15), (17), and (18) that

$$\mathbf{Z}^{(m,s)} = \left(\mathbf{I} + \mathbf{\Gamma}^{(m,s)}\right) \left(\mathbf{I} - \mathbf{\Gamma}^{(m,s)}\right)^{-1} \tag{19}$$

$$\text{and} \quad \mathbf{\Gamma}^{(m,s)} = \left(\mathbf{Z}^{(m,s)} - \mathbf{I}\right) \left(\mathbf{Z}^{(m,s)} + \mathbf{I}\right)^{-1}, \tag{20}$$

where $\mathbf{I}$ is the identity matrix. From (10) we obtain

$$\mathbf{u}^{(m,u,\pm)} = \exp\left(\pm i \mathbf{K}^{(m)}\right) \mathbf{u}^{(m,l,\pm)}. \tag{21}$$

Then (21) and (18) yield

$$\mathbf{\Gamma}^{(m,u)} = \exp\left(-i \mathbf{K}^{(m)}\right) \mathbf{\Gamma}^{(m,l)} \exp\left(-i \mathbf{K}^{(m)}\right), \tag{22}$$

which may be combined with (19) and (20) to yield

$$\mathbf{Z}^{(m,u)} = \left[\cos\left(\mathbf{K}^{(m)}\right) \mathbf{Z}^{(m,l)} + i \sin\left(\mathbf{K}^{(m)}\right)\right] \left[i \sin\left(\mathbf{K}^{(m)}\right) \mathbf{Z}^{(m,l)} + \cos\left(\mathbf{K}^{(m)}\right)\right]^{-1} \tag{23}$$

This formula also holds if the impedances $\mathbf{Z}^{(m,s)}$ are replaced by the admittances $\left(\mathbf{Z}^{(m,s)}\right)^{-1}$. The formula must be written in a different form to handle evanescent waves in thick slices correctly.

Let us assume that we have discrete spatial representations $\vec{E}_{(\vec{g},p)}^{(m)}(\vec{r})$ and $\vec{H}_{(\vec{g},p)}^{(m)}(\vec{r})$ of the transverse E-and H-fields of each BWEF in slice no. m. These representation may be considered to be matrices $\mathbf{O}^{(m;E)}$ and $\mathbf{O}^{(m;H)}$ with matrix elements $O_{(\vec{r},c),(\vec{g},p)}^{(m;E)}$ and $O_{(\vec{r},c),(\vec{g},p)}^{(m;H)}$, respectively, with $\vec{r}$ running over the spatial positions and c representing either one of the two transverse field components. Point matching of the transverse E- and H-fields across the interface between slice m and slice $m+1$ yields

$$\mathbf{O}^{(m+1;E)}\mathbf{u}^{(m+1,l,E)} = \mathbf{O}^{(m;E)}\mathbf{u}^{(m,u,E)} \tag{24}$$

$$\text{and} \quad \mathbf{O}^{(m+1;H)}\mathbf{u}^{(m+1,l,H)} = \mathbf{O}^{(m;H)}\mathbf{u}^{(m,u,H)}, \tag{25}$$

or

$$\mathbf{u}^{(m+1,l,E)} = \left[\mathbf{O}^{(m+1;E)}\right]^{-1}\mathbf{O}^{(m;E)}\mathbf{u}^{(m,u,E)} = \mathbf{O}^{(m+1,m;E)}\mathbf{u}^{(m,u,E)} \tag{26}$$

$$\text{and} \quad \mathbf{u}^{(m+1,l,H)} = \left[\mathbf{O}^{(m+1;H)}\right]^{-1}\mathbf{O}^{(m;H)}\mathbf{u}^{(m,u,H)} = \mathbf{O}^{(m+1,m;H)}\mathbf{u}^{(m,u,H)}, \tag{27}$$

defining the slice interface coupling matrices $\mathbf{O}^{(m+1,m;E)}$ and $\mathbf{O}^{(m+1,m;H)}$.

Just like in (11; 9), recursion relations may then be deduced for the impedances:

$$\begin{aligned}\mathbf{Z}^{(m+1,l)} &= \mathbf{O}^{(m+1,m;E)}\mathbf{Z}^{(m,u)}\mathbf{O}^{(m,m+1;H)} = \\ &= \mathbf{O}^{(m+1,m;E)}\left[\cos\left(\mathbf{K}^{(m)}\right)\mathbf{Z}^{(m,l)} + i\sin\left(\mathbf{K}^{(m)}\right)\right]\left[i\sin\left(\mathbf{K}^{(m)}\right)\mathbf{Z}^{(m,l)} + \cos\left(\mathbf{K}^{(m)}\right)\right]^{-1}\mathbf{O}^{(n}\end{aligned}$$

This equation is easily inverted to yield $\mathbf{Z}^{(m,l)}$ expressed by $\mathbf{Z}^{(m+1,l)}$.

Let waves be incident from the bottom. Then we have no waves coming down through the top slice, and no fields that decay exponentially as we go down from the top. We have only the transmitted upward waves and the evanescent fields from the bottom of the top slice. Now it is obvious why these fields belong together in the definitions of $\mathbf{Z}^{(m,s)}$ and $\mathbf{\Gamma}^{(m,s)}$. That choice yields the simple boundary condition

$$\mathbf{\Gamma}^{(M,l)} = 0 \ \text{ and } \mathbf{Z}^{(M,l)} = \mathbf{I}\ . \tag{30}$$

Recursive application of (29) then allows us to compute the impedance matrix $\mathbf{Z}^{(1,l,-)}$ at the bottom of the bottom slice. The reflection coefficient matrix $\mathbf{\Gamma}^{(1,l,-)} = \left(\mathbf{Z}^{(1,l,-)} - \mathbf{I}\right)\left(\mathbf{Z}^{(1,l,-)} + \mathbf{I}\right)^{-1}$, given by (??) for $m = 1$, then yields the reflected waves resulting from an incoming wave.

0.0.3 Discussion

The formalism above may be used to analyze a number of planar multilayer transmission or reflection filters incorporating photonic crystal layers. Reflection and transmission coefficients for the optical plane waves may be calculated, as a function of optical frequency, angle of incidence with respect to the surface normal, and polarization (TE or TM). Polarization conversion in reflection and transmission may be investigated . Each layer in the multilayer filter may be a photonic crystal. There is a requirement in that all layers have to have the same crystal lattice structure, i.e., the same lattice constants and the same angle between the lattice axes. Any guided resonances of the photonic crystal structure may be found by investigation of the reflection coefficient matrix

$\mathbf{\Gamma}^{(1,l,-)}$ of the bottom slice. The resonances may be found by analyzing the frequency dependence of the elements of this matrix that correspond to travelling (non-evanescent) incoming and reflected waves. If the lattice constants of the photonic crystal are sufficiently small compared to the wavelength, there is only one incoming and one reflected wave possible.

The number of BW components needed in the field expansion for a given transverse spatial resolution is roughly equal to two (polarizations) times the product of the two lattice periods of the PC divided by the spatial resolution squared. With desktop computers, if a few minutes of processing time is allowed, matrices with a dimension of over a thousand may be manipulated. For frequencies not too far above the lowest photonic bandgaps, the optical wavelength in any of the constituent materials of the PC is not much smaller than any of the two lattice periods of the PC. Then a resolution of a small fraction of a wavelength may easily be obtained on a desktop computer. This resolution is necessary to reproduce the divergence of the electric field at edges (2; 4), and reach convergence for the calculation of BW fields. In calculations with such a resolution not too far above the lowest bandgaps, most of the BW components in the expansions (7) are evanescent BWs, *i.e.*, with imaginary $k_{\vec{g},p}^{(m)}$.

As already pointed out in (11; 9; 10), to get a numerically well behaved recursion relation for propagation of the Bloch wave (BW) amplitudes and derivatives (the u's) through the slices, it is important not to work with the u's directly, but rather with the impedance matrices $\mathbf{Z}^{(m,s)}$, as in (29). It should also be mentioned that an equally well behaved formulation may be obtained in terms of the scattering matrices $\mathbf{\Gamma}^{(m,s)}$.

0.0.4 Acknowledgements

Helpful discussions with Professor Reinhold Pregla at the FernUniversität Hagen are gratefully acknowledged.

0.0.5 References:

References

[1] D. Marcuse, *Theory of Dielectric Optical Waveguides*, second edition, Academic Press, San Diego, 1991.

[2] J. van Bladel, *Singular electromagnetic fields and sources*, Ch. 4, Clarendon Press, Oxford, 1991.

[3] W. Schlosser and H. G. Unger, "Partially filled waveguides and surface waveguides of rectangular cross section," *Advances in Microwaves*, pp. 319-387, Academic, New York, 1966.

[4] A. S. Sudbø , "Why are accurate computations of mode fields in rectangular dielectric waveguides difficult?" *J. Lightwave Technol.*, Vol. 10, pp. 418-419, 1992.

[5] T. Itoh (editor), *Numerical techniques for microwave and millimeter-wave passive structures*, Wiley, New York, 1988.

[6] R. Sorrentino, “Transverse resonance technique,” Ch. 11 in Itoh’s book (5).

[7] R. Pregla and W. Pascher, “The method of lines,” Ch. 6 in Itoh’s book (5).

[8] A. S. Sudbø , “Film mode matching: A versatile method for mode field calculations in dielectric waveguides,” *Pure Appl. Opt. (J. Europ. Opt. Soc. A)*, Vol. 2, pp. 211-233, 1993.

[9] A. S. Sudbø , “Improved formulation of the film mode matching method for mode field calculations in dielectric waveguides,” to be published in *Pure Appl. Opt. (J. Europ. Opt. Soc. A).*

[10] R Pregla, A Sudbø, and Ph. Sewell, “Mode solvers and related methods,” Ch. 1 in G Guekos, Ed., “*Photonic Devices for Telecommunications,*” Springer, Berlin 1998.

[11] U. Rogge and R. Pregla, “Method of lines for the analysis of dielectric waveguides,” *J. Lightwave Technol.*, Vol. 11, pp. 2015-2020, 1993.

[12] M. S. Stern, P. C. Kendall, and P. W. A. McIlroy, “Analysis of the spectral index method for vector modes of rib waveguides,” *IEE Proc. J*, Vol. 137, pp. 21-26, 1990.

[13] W. Pascher and R. Pregla, “Analysis of curved optical waveguides by the vectorial method of lines,” *17th European Conference on Optical Communication (ECOC ’91),* paper TuB5-5, Paris, Sept 9-12, 1991.

[14] A. Dreher and R. Pregla, “Analysis of planar waveguides with the method of lines and absorbing boundary conditions,” *IEEE Microw. Guided Wave Lett.*, Vol. 1, pp. 138-140, 1991.

[15] K.A. Zaki, S.W. Chen, and C.Chen, ”Modeling discontinuities in dielectric-loaded waveguides,” IEEE Trans. Microwave Theory Tech., vol. 36, pp. 1804, 1988.